BMC Plant Biology

RESEARCH

Open Access

RGB-UAV-based phenotyping reveals the influence of planting density on physiological traits, biomass, and yield in buckwheat

E. M. B. M. Karunathilake[1,11†], Sheikh Mansoor[2,12†], Seong Mun Lee[3], Gyung Deok Han[4], Tuan Ngoc Nguyen[5], Hang T. T. Nguyen[6], Piya Kittipadakul[7], Supachai Vuttipongchaikij[8], Manh Cuong Do[9,10*] and Yong Suk Chung[1*]

Abstract

Accurate estimation of crop yield and biomass using UAV-based remote sensing is influenced by flight altitude, plant density, canopy structure, vegetation index (VI) selection, and crop growth stage. This study evaluated how the joint optimization of these factors influences biomass and yield prediction in common buckwheat (*Fagopyrum esculentum* Moench var. 'Yangjeol'). Field experiments were conducted using broadcast seeding and drill seeding at four row spacings (12.5, 20, 30, and 40 cm) following the complete Latin square design. UAV RGB imagery was acquired at the third-leaf and full-flowering stages from 30, 50, and 60 m altitudes, and vegetation indices Excess Green Index (ExG), Green Leaf Index (GLI), and Normalized Green–Red Difference Index (NGRDI)were extracted. ANOVA with Tukey's HSD revealed significant variations in biomass and yield traits among sowing treatments ($p < 0.005$). The highest fresh weight was recorded under drill seeding at 12.5 cm spacing, while seed weight was consistently higher under all drill seeding treatments compared with broadcast seeding. The number of seeds per plant peaked under 40 cm spacing, indicating a trade-off between planting density and reproductive output. Strong and significant correlations between vegetation indices and ground-measured traits were observed ($r = 0.82–0.98$), but these relationships were highly dependent on growth stage, sowing configuration, and UAV altitude. The third-leaf stage under broadcast seeding and full flowering stage under drill seeding at 20 cm spacing showed the strongest and most consistent VI–trait associations. Among UAV altitudes, 50 m provided the most stable predictive performance across traits. ExG and GLI exhibited more consistent relationships with biomass and yield parameters than NGRDI. These findings demonstrate that no single UAV altitude, vegetation index, or growth stage is universally optimal. Instead, coordinated optimization of UAV operational parameters and sowing configurationsubstantially improves the reliability of UAV-based yield and biomass estimation in buckwheat.

Keywords Buckwheat, Remote sensing, Phenotyping, Sowing method, Vegetation index, Yield prediction

†E. M. B. M. Karunathilake and Sheikh Mansoor equally contributed equally to this work.

*Correspondence:
Manh Cuong Do
domanhcuong2@duytan.edu.vn
Yong Suk Chung
yschung@jejunu.ac.kr

Full list of author information is available at the end of the article

© The Author(s) 2026. **Open Access** This article is licensed under a Creative Commons Attribution-NonCommercial-NoDerivatives 4.0 International License, which permits any non-commercial use, sharing, distribution and reproduction in any medium or format, as long as you give appropriate credit to the original author(s) and the source, provide a link to the Creative Commons licence, and indicate if you modified the licensed material. You do not have permission under this licence to share adapted material derived from this article or parts of it. The images or other third party material in this article are included in the article's Creative Commons licence, unless indicated otherwise in a credit line to the material. If material is not included in the article's Creative Commons licence and your intended use is not permitted by statutory regulation or exceeds the permitted use, you will need to obtain permission directly from the copyright holder. To view a copy of this licence, visit http://creativecommons.org/licenses/by-nc-nd/4.0/.

Introduction

Precision agriculture increasingly integrates unmanned aerial vehicles (UAVs) as vital tools for monitoring crop growth, assessing vigor, and accurately estimating yield and biomass at large scales [1–3]. UAVs generate high-resolution aerial imagery that, when combined with vegetation indices (VIs), enables non-destructive and cost-effective evaluation of crop performance over extensive fields [4]. The precision of UAV-based crop measurements is influenced by multiple tightly interrelated factors, including UAV flight height, sowing methods, planting interval, choice of VIs, and crop developmental stages [5, 6].

UAV flight height plays a pivotal role in determining image spatial resolution and the capacity to capture detailed structural traits, such as canopy cover, plant height, and leaf distribution [5]. Lower flight altitudes, typically between 15 and 50 m, enhance ground sampling distance and improve detection of fine-scale features, especially critical during early crop growth stages when plants are smaller and more variable. However, such low altitudes require more image captures, leading to increased data processing times and operational costs. Conversely, higher flight altitudes facilitate faster coverage of large areas but suffer from reduced spatial resolution, which can limit the accuracy of early-stage biomass and height estimations [7–9].

Sowing methods and planting intervals govern canopy density, uniformity, and spacing, which directly affect the spectral signatures recorded by UAV sensors [10]. Alterations in canopy structure influence the responsiveness and saturation thresholds of common vegetation indices such as Excess Green Index (ExG), Green Leaf Index (GLI), and Normalized Green–Red Difference Index (NGRDI) [11]. These indices serve as spectral proxies for plant physiological status and biomass but vary in sensitivity depending on crop density and developmental stage [12].

Crop phenology profoundly impacts the utility of UAV-derived VIs. Measurements taken during the early leaf development stage primarily reveal initial vigor and biomass accumulation but typically correlate less strongly with final yield components [12]. In contrast, indices obtained during the flowering stage tend to exhibit higher correlations with critical yield traits such as fresh weight, seed number, and seed weight [13, 14]. Empirical evidence suggests that integrating imaging at these phenological stages, along with selecting optimal UAV flight heights and adjusting sowing strategies, particularly through drill seeding at narrower planting intervals, maximizes the association strength between VIs and yield traits [15, 16].

Importantly, sowing method and planting density are primarily determined by agronomic considerations such as yield optimization, mechanization efficiency, weed suppression, and resource-use efficiency, rather than by remote sensing requirements [7, 10]. Farmers do not modify planting configurations to improve UAV image correlations; instead, UAV-based monitoring systems must adapt to existing agronomic practices [2, 17]. Therefore, understanding how different sowing configurations influence canopy reflectance and VI responsiveness is essential for developing robust remote sensing protocols that remain reliable under practical field conditions.

We selected *Fagopyrum esculentum* Moench var. 'Yangjeol', a Korean-bred cultivar adapted to the temperate monsoon climate characterized by short growing seasons and cool autumn conditions. Its early maturation cycle (approximately 75–80 days) makes it well-suited to Korean upland farming systems. 'Yangjeol' is agronomically valued for its uniform plant height (~ 110 cm), strong stem rigidity conferring lodging resistance, relatively large seed size, and resistance to major fungal diseases such as leaf spot caused by *Alternaria alternata*. In addition, it is an important food crop due to its high rutin content and superior flour quality, widely used for traditional memil-guksu (buckwheat noodles) and as a gluten-free nutritional resource [10, 18–20].

Recent advances in precision agriculture have increasingly incorporated machine learning, IoT, and data-driven frameworks to enhance crop monitoring and yield prediction. For instance, Reddy et al. [21] demonstrated that Naïve Bayes achieved higher prediction accuracy (88%) compared to convolutional neural networks (82%) for crop yield estimation, highlighting the potential of lightweight models in agricultural applications. Similarly, Balaji et al. [22] developed an IoT-driven crop recommendation system integrating soil and weather data using XGBoost, achieving up to 99% prediction accuracy and demonstrating the effectiveness of real-time environmental data integration. In another approach, Vinayagam et al. [23] proposed a blockchain-enabled crop monitoring system using InterPlanetary File System (IPFS), which improved data integrity and scalability while achieving high accuracy (98%) and confidentiality (99.8%). Emerging techniques such as quantum-based biophotonic analysis have also been explored for crop quality assessment, offering novel non-invasive monitoring approaches, although challenges remain in standardization and environmental adaptability Shoba et al. [24].

Despite these advancements, several limitations persist in existing studies. Many machine learning-based approaches rely on controlled datasets or static conditions, limiting their applicability under real-field variability. IoT-based systems, while highly accurate, often depend on continuous sensor infrastructure, increasing implementation cost and complexity [25]. Similarly, blockchain-based frameworks emphasize data integrity

and traceability but do not directly address canopy-level variability or spectral response dynamics relevant to crop phenotyping [26]. Furthermore, most existing models focus primarily on algorithmic optimization while overlooking the influence of agronomic factors such as sowing configuration, canopy structure, and phenological stage on data quality and predictive performance.

In contrast, UAV-based remote sensing provides a scalable and non-invasive alternative for field-level monitoring; however, its predictive reliability remains highly sensitive to operational and agronomic conditions [11, 15]. Previous studies have typically evaluated individual factors such as flight altitude or vegetation indices in isolation, without systematically integrating their interactions with crop management practices [8]. Therefore, a critical research gap exists in developing an integrated framework that simultaneously optimizes UAV acquisition parameters, vegetation indices, phenological timing, and agronomic configurations under realistic field conditions.

The primary purpose of this investigation was to develop an integrated, multi-factorial framework for accurately estimating the seed yield and biomass of common buckwheat (*Fagopyrum esculentum* Moench) using VIs derived from UAV imagery. Specifically, the study aimed to systematically quantify and optimize the interactive effects of four critical variables such as UAV flight altitude, sowing method/planting density, the selection of the appropriate VI, and the timing of image acquisition (with two selected crop phenological stages), to establish robust, predictive remote sensing protocols. By determining the optimal combination of these operational and agronomic factors, this research sought to significantly enhance the precision and reliability of UAV-based crop monitoring and yield forecasting within precision agriculture systems.

Materials and methods

Plant materials

The *F. esculentum* Moench variety 'Yangjeol', obtained from the Agricultural Genetic Resources Centre, National Institute of Agricultural Sciences, Rural Development Administration, South Korea, was used in this study.

Buckwheat was planted at the end of August 2023 at the Buckwheat Field of the Jeju Special Self-Governing Province Agricultural Research and Extension Services, located at 992–2, Sanggwi-ri, Aewol-eup, Jeju-si, Jeju-do, Republic of Korea (33° 44′ N, 126° 40′ E; altitude 183 m). Two sowing methods were employed: broadcast seeding and drill seeding. Broadcast seeding was conducted by uniformly distributing seeds over the soil surface followed by light raking to ensure partial soil coverage. Drill seeding was performed by placing seeds manually in rows at predetermined spacing intervals (12.5, 20, 30, and 40 cm between rowsnd 5 cm between plants), ensuring controlled plant-to-plant spatial arrangement. These spacing treatments represented different planting densities, which were used to evaluate the effect of crop spatial configuration on canopy development and yield-related traits (Table 1). Each treatment plot measured 15 m^2 (3 m × 5 m), and the experiment was arranged in a 5 × 5 complete Latin square design (Fig. 1). The amount of seed required for each treatment, including both sowing methods and spacing variations, is summarized in Table 1.

During the growing season, the mean air temperature ranged from 27.5 °C in August to 19 °C in October, 2023, total precipitation was recorded as high with late-summer rainfall events. These conditions are representative of the typical cool-temperate monsoon climate of Jeju Island, which influences buckwheat growth and development. Meteorological data for the experimental period (August—October, 2023) were obtained from the nearest weather station of the Korea Meteorological Administration.

Table 1 Seed Amount Required for Each Treatment, broadcast and drill seedling (DS)

Sowing methods	Seed amount/Plot (kg)	Seed amount/Treatment (kg)
Broadcast seeding	0.150	0.750
DS12.5 (Drill seedling 12.5 cm)	0.105	0.525
DS20 (Drill seedling 20 cm)	0.090	0.450
DS30 (Drill seedling 30 cm)	0.060	0.300
DS40 (Drill seedling 40 cm)	0.045	0.225

Image acquisition

The images analyzed in this study were acquired at the third leaf stage (8th September 2023) and the full flowering stage (21st September 2023) at three different altitudes 30, 50, and 60 m. The third leaf stage refers to the point at which the first, second, and third leaves are fully expanded at each node, and the full flowering stage is characterized by open flowers being present in most inflorescences. Image acquisition was conducted using an UAV, specifically the MATRICE 300 RTK drone (Model: M300, DJI, China), equipped with a 45 MP RGB camera (effective pixels: 45 MP; pixel size: 4.4 μm), which was flown at altitudes of 30 m, 50 m, and 60 m, with an 80% image overlap rate. Flight altitudes were selected to balance spatial resolution and field coverage. Lower altitudes (30 m and 50 m) provide higher spatial resolution and were therefore more suitable for detailed yield estimation, including pixel-based canopy analysis. The higher altitude (60 m) allowed broader area coverage

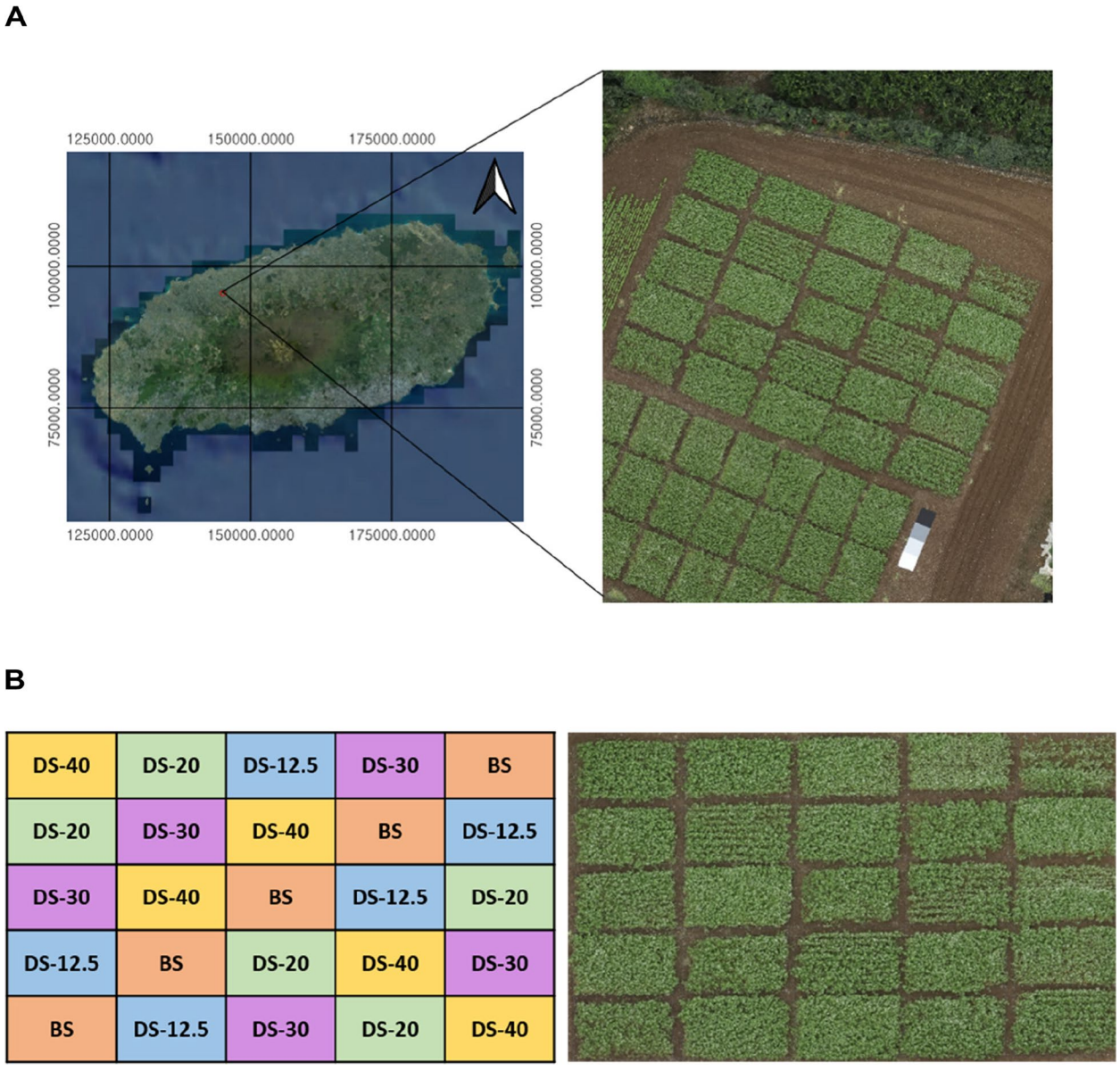


Fig. 1 The field location and experimental design of the study field. Field location in Jeju Island (**A**); Experimental design of the study field (**B**). *DS—40: Drill Seeding at 40 × 5 cm spacings, DS—30: Drill Seeding at 30 × 5 cm spacings, DS—20: Drill Seeding at 20 × 5 cm spacings, DS – 12.5: Drill Seeding at 12.5 × 5 cm spacings, BS: Broadcast Seeding*

while maintaining sufficient image quality for vegetation index extraction. In addition, all flight heights were chosen in compliance with the legal UAV operational regulations in the Republic of Korea [5, 27, 28]. All images were captured between 2:00 PM and 3:00 PM local time under clear sky conditions to minimize variation in lighting. A standard radiometric calibration tarp with uniform reflectance, provided by Group 8 Technology, was included in each image as a reference during acquisition.

Data collection

Plants were sampled at full maturity on 31 st October 2023. In each plot, ten plants were randomly selected to measure total fresh weight of plants (FW), seed weight (SW), number of seeds per plant (NS), plant height (PH). All above-ground plant material within each plot was harvested by cutting at the soil surface for assessment. The total fresh weight was immediately measured in the laboratory using a digital balance to minimize moisture loss, and all harvested biomass within each plot boundary was included in the measurement. To collect seeds, harvested plants were manually threshed, and debris was carefully removed. The cleaned seeds were weighed using a precision balance and subsequently air-dried under ambient laboratory conditions (room temperature, well-ventilated area) until a constant weight was achieved (no

further change in weight after consecutive measurements over 24 h). Seed counts were conducted at the individual plant level and then averaged to obtain mean values for each plot for statistical analysis.

Image processing

Raw RGB images were preprocessed before analysis to improve data quality. The preprocessing workflow included geometric distortion correction and radiometric calibration, both essential for ensuring the accuracy and consistency of image-derived data. Acquired images showed a barrel distortion, a type of radial distortion that is caused by the camera lens characteristics [29]. This radial distortion was rectified using a Python program (version 3.11.9) (Fig. 2), which has been developed using the checkerboard method [30].

The process of radiometric calibration is essential for equalizing light conditions in remote sensing imagery, which can vary significantly due to weather and time of day. This procedure also ensures the reliability of the data [9, 31]. This step was performed using the Empirical Line Method (ELM) to convert digital number (DN) values to surface reflectance using the uniform tarp reference panel with known reflectance values, which was placed within the field of view during image acquisition. For each spectral band, a linear regression (best-fit equation) was established between the DN values of the reference panel and its known reflectance, and the resulting calibration coefficients were applied to the entire image to obtain reflectance-corrected data. This procedure minimizes illumination variability caused by changing weather and acquisition time, thereby ensuring consistency and comparability of spectral measurements across flights [31, 32].

Following preprocessing, the images were analyzed using ImageJ software. During this stage, the RGB images were decomposed into three separate color channels: red (R), green (G), and blue (B). Pixel intensity values for each treatment plot were extracted from each channel using the region of interest (ROI) tool in ImageJ. Based on these intensity values, VIs were calculated, including the Excess Green. Index (ExG) (Eq. 1), the Green Leaf Index (GLI) (Eq. 2), and the Normalized Green–Red Difference Index (NGRDI) (Eq. 3) [33, 34].

$$ExG = 2 \times g - b - r; r = \frac{R}{R+G+B}, \quad g = \frac{G}{R+G+B}, b = \frac{B}{R+G+B} \tag{1}$$

$$GLI = \frac{2 \times g - b - r}{2 \times g + b + r}; r = \frac{R}{R+G+B}, \quad g = \frac{G}{R+G+B}, b = \frac{B}{R+G+B} \tag{2}$$

$$NGRDI = \frac{G-R}{G+R} \tag{3}$$

where R, G, and B are the reflectance of red, green, and blue bands, respectively. These three Vis were deliberately selected based on their documented robustness and complementary sensitivity to canopy characteristics under RGB imaging conditions. ExG was included due to its demonstrated stability in monitoring vegetative growth and its strong responsiveness to canopy greenness across developmental stages [35, 36]. GLI and NGRDI were selected for their effectiveness in discriminating green vegetation from soil and background noise in high-resolution UAV imagery. In particular, GLI has been reported to exhibit relative resistance to variable illumination conditions, making it suitable for field-based UAV applications. NGRDI enhances the green–red contrast, thereby emphasizing vegetation greenness and serving as a proxy for phenological progression and chlorophyll dynamics. Collectively, these indices provide a balanced framework for evaluating canopy vigor, structural development, and greenness using standard RGB sensors without requiring multispectral instrumentation [8, 15, 37].

Statistical analysis

All statistical analyses were conducted using R software (version 4.4.1; R Core Team, 2013). Prior to analysis, data were aggregated at the plot level, and mean values per treatment replicate were used as the experimental units. Assumptions of normality and homogeneity of variance were evaluated using the Shapiro–Wilk test and Levene's test, respectively. As the data met the assumptions of normal distribution and homoscedasticity, parametric tests were applied.

To examine differences in bimass and yield traits among sowing methods, one-way analysis of variance (ANOVA) was performed, followed by Tukey's honest significant difference (HSD) post hoc test to determine pairwise differences between treatment means. To evaluate relationships between ground-measured biomass and yield traits (FW, SW, NS, PH) and VIs derived from UAV imagery, Pearson correlation analyses were conducted separately for each sowing method and UAV altitude (30, 50, and 60 m). Linear regression models were further fitted to quantify the predictive relationships between selected VIs and yield-related traits. All statistical tests were considered significant at $p < 0.05$. Data processing and visualization were performed using the tidyverse [38], ggpubr [39], car [40], GGally [41], stats, and agricolae [42] for ANOVA and Tukey HSD analysis.

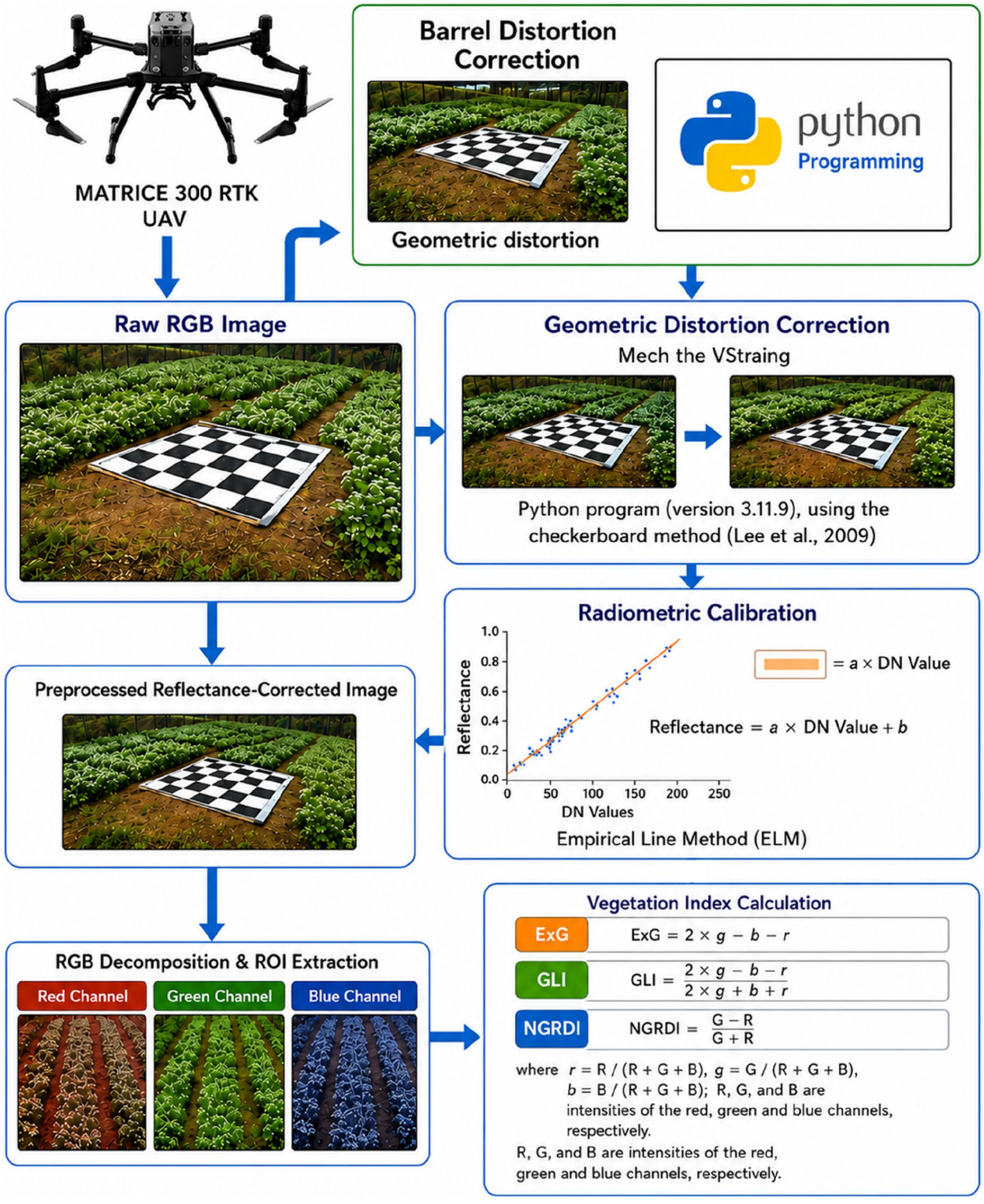


Fig. 2 Workflow for processing UAV-acquired RGB imagery and deriving vegetation indices. *DN: digital numbers; ExG: Excess Green Index; GLI: Green Leaf Index; NGRDI: Normalized Green–Red Difference Index*

Results

Buckwheat biomass and yield traits by sowing methods

The biomass and yield-related traits were significantly influenced by the sowing methods (Table 2). Drill seeding at 12.5 cm spacing (DS12.5), Broadcast Seeding (BS) and Drill Seeding at 40 cm spacing (DS40), while Drill Seeding at 20 cm spacing (DS20) and Drill Seeding at 30 cm spacing (DS30). Fresh weight (FW) differed markedly among treatments ($F = 6.45$, $p < 0.001$), ranging from 758.40 to 1102.40 g m^{-2}. Broadcast seeding (BS) produced the lowest FW (758.40 ± 54.05 g m^{-2}), whereas drill seeding at 12.5 cm spacing (DS12.5) resulted in the highest FW (1102.40 ± 65.09 g m^{-2}). Similarly, DS20 and DS30 also recorded significantly greater FW than BS, indicating that drill seeding substantially enhanced biomass accumulation compared with broadcast establishment. Although DS40 showed intermediate FW values (953.60 ± 30.04 g m^{-2}), it remained statistically comparable to both BS and the other drill-seeded treatments.

Seed weight (SW) also varied significantly among sowing methods ($F = 3.88$, $p < 0.001$). The lowest SW was observed under BS (165.87 ± 11.71 g m^{-2}), while all drill-seeded treatments produced significantly higher SW values, ranging from 209.07 to 214.13 g m^{-2}. Among these, DS12.5 recorded the maximum SW (214.13 ± 13.41 g m^{-2}), although no significant differences were detected among the drill-seeded treatments. The consistently greater SW under drill seeding suggests improved vegetative growth and dry matter accumulation relative to broadcast seeding.

The number of seeds (NS) was significantly affected by sowing geometry ($F = 4.61$, $p < 0.001$). DS40 produced the highest NS (83.48 ± 6.30), significantly exceeding the values recorded for the other treatments. In contrast, DS20 exhibited the lowest NS (61.58 ± 3.93). BS, DS12.5, DS20, and DS30 showed statistically similar NS values, indicating that wider row spacing primarily contributed to enhanced seed production. The increased NS under DS40 may be attributed to reduced inter-plant competition and improved allocation of assimilates toward reproductive growth.

Plant height (PH) showed the strongest treatment response among all measured traits ($F = 10.07$, $p < 0.001$). The shortest plants were observed under BS and DS12.5 (0.70 ± 0.01 m), whereas DS20 produced significantly taller plants (0.76 ± 0.01 m). Intermediate values were recorded for DS30 and DS40, both of which were significantly taller than BS. These findings indicate that drill seeding, particularly at moderate row spacing, promoted vertical growth, likely due to improved light interception and resource utilization.

The drill seeding methods consistently outperformed broadcast seeding for most biomass and yield-related traits. Narrow to moderate drill spacings (12.5–30 cm) favored biomass production, whereas wider spacing (40 cm) enhanced seed number. The significant differences identified by Tukey's HSD test further demonstrate the strong influence of sowing geometry on crop growth and productivity.

Table 2 ANOVA results of buckwheat biomass and yield traits by sowing methods

Seedling methods[x]	Traits[y]			
	FW (g m^{-2})[z]	SW (g m^{-2})[z]	NS[z]	PH (m)[z]
BS	758.40 ± 54.05[a]	165.87 ± 11.71[a]	72.22 ± 3.54[a]	0.70 ± 0.01[a]
DS12.5	1102.40 ± 65.09[b]	214.13 ± 13.41[b]	62.96 ± 1.76[a]	0.70 ± 0.01[a]
DS20	1057.74 ± 62.17[b]	209.07 ± 11.32[b]	61.58 ± 3.93[a]	0.76 ± 0.01[b]
DS30	1030.67 ± 47.88[b]	210.13 ± 7.82[b]	69.82 ± 3.54[a]	0.74 ± 0.01[b]
DS40	953.60 ± 30.04[ab]	213.07 ± 6.18[b]	83.48 ± 6.30[b]	0.73 ± 0.01[b]
F-value	6.45	3.88	4.61	10.07
p-value	$p < 0.001$	$p < 0.001$	$p < 0.001$	$p < 0.001$

[x]BS and DS indicate broadcast seeding and drill seeding, respectively

[y]FW, SW, NS, and PH indicate fresh weight, seed weight, number of seeds, and plant heights, respectively

[z]Mean ± Standard Error. Different letters within columns indicate significant differences (Tukey's HSD, $p < 0.05$, n = 10 per plot)

Correlation and determination analysis of vegetation indices

The relationships between vegetation indices (VIs) and biomass and yield traits varied according to growth stage, sowing method, and UAV flight altitude (Table 3 and Table S1). At the third leaf stage, FW and SW under BS showed strong positive correlations with all RGB-based indices at 50 m altitude, indicating that this altitude provided optimal image quality for detecting early vegetative vigor. In contrast, during the full flowering stage, significant relationships were mainly observed under drill seeding at 20 cm spacing (DS20), where FW was strongly correlated with all three VIs at 50 m altitude, while seed weight (SW) showed significant associations with ExG and GLI. Fresh weight (FW) showed the strongest and most consistent associations with vegetation indices across all evaluated conditions. At 30 m altitude under broadcast seeding (BS), NGRDI measured at the third leaf (TL) stage exhibited a very strong positive correlation with FW ($r = 0.96$, $R^2 = 0.90$), indicating that nearly 90% of the variation in FW could be explained by NGRDI values. Similarly, NGRDI at the full flowering (FF) stage also maintained a strong relationship with FW ($r = 0.92$, $R^2 = 0.80$), although the correlation strength declined slightly compared with the vegetative stage. These findings suggest that early vegetative canopy characteristics captured by NGRDI were highly sensitive to biomass accumulation under BS conditions.

Under drill seeding at 20 cm spacing (DS20), correlations between FW and vegetation indices were

Table 3 Pearson correlation coefficients (r) and coefficients of determination (R^2) between vegetation indices and biomass and yield traits under different UAV altitudes and Sowing methods

Altitude (m)		Sowing Methods[x] (cm)	ExG				GLI				NGRDI			
			TL[y]		FF		TL		FF		TL		FF	
			r	R^2	r	R^2	r	R^2	r	R^2	r	R^2	r	R^2
FW[z]	30 m	BS							0.96**	0.90	0.92*	0.80		
		DS20			0.96**	0.90							0.96*	0.88
	50 m	BS	0.95*	0.86			0.95*	0.87			0.94*	0.84		
		DS20			0.98**	0.94			0.98**	0.94			0.96**	0.90
	60 m	DS20			0.92*	0.79			0.92*	0.79				
NS	60 m	DS30			0.82*	0.59			0.82	0.60				
SW	30 m	DS20											0.91*	0.78
	50 m	BS	0.96*	0.89			0.96**	0.90			0.94*	0.86		
		DS20			0.89*	0.72			0.89*	0.72				

Blank cells and omitted columns such as missing sowing methods and plant height indicate no association

*Significant at $p < 0.05$

**Significant at $p < 0.01$

[x]BS and DS indicate broadcast seeding and drill seeding, respectively

[y]TL and FF indicate the third leaf stage and the full flowering stage, respectively

[z]FW, NS, and SW indicate fresh weight (g m^{-2}), number of seeds, and seed weight (g m^{-2}), respectively

consistently stronger than those observed under BS. At 30 m altitude, GLI measured during the FF stage showed a very strong positive correlation with FW (r = 0.96, R^2 = 0.90), while NGRDI at FF produced similarly high predictive performance (r = 0.96, R^2 = 0.88). At 50 m altitude, the relationships further strengthened, with GLI at FF exhibiting the highest correlation observed in the study (r = 0.98, R^2 = 0.94). A similarly strong relationship was detected for NGRDI at FF (r = 0.96, R^2 = 0.90). These results demonstrate that under optimized sowing geometry, vegetation indices derived during the reproductive stage can accurately estimate biomass production even at moderate UAV flight altitudes.

The ExG index also performed well in predicting FW, particularly at 50 m altitude. Under BS conditions, ExG at the TL stage showed a strong positive correlation with FW (r = 0.95, R^2 = 0.86), while GLI and NGRDI recorded comparable relationships (r = 0.95 and 0.94, respectively). The similarity among these indices suggests that all three vegetation indices effectively captured canopy greenness and structural characteristics associated with crop biomass.

However, correlations generally became stronger under drill seeding compared with broadcast seeding, indicating that more uniform canopy distribution under drill sowing improved spectral response consistency. At the higher altitude of 60 m, the predictive performance of vegetation indices declined slightly. Under DS20, GLI at FF maintained a significant positive relationship with FW (r = 0.92, R^2 = 0.79). Although still statistically significant, the lower R^2 compared with 30 and 50 m flights indicates some reduction in canopy detail and spectral sensitivity at greater image acquisition heights. This suggests that lower to moderate UAV altitudes were more effective for accurately detecting crop biomass variability.

The number of seeds (NS) exhibited comparatively weaker relationships with vegetation indices than FW. At 60 m altitude under DS30, GLI at FF showed a moderate positive correlation with NS (r = 0.82, R^2 = 0.59), whereas the corresponding relationship at the TL stage remained similar (r = 0.82, R^2 = 0.60) but lacked statistical significance. The lower coefficients observed for NS compared with FW indicate that reproductive traits were less directly associated with canopy spectral characteristics, particularly at higher UAV altitudes.

Seed weight (SW) also demonstrated significant associations with vegetation indices, particularly under drill seeding conditions. At 30 m altitude under DS20, NGRDI at FF exhibited a strong positive correlation with SW (r = 0.91, R^2 = 0.78), indicating that reproductive-stage canopy reflectance effectively explained variation in grain production. Similarly, at 50 m altitude under BS, ExG and GLI at TL showed very strong correlations with SW (r = 0.96, R^2 = 0.89 and r = 0.96, R^2 = 0.90, respectively),

while NGRDI also maintained a strong relationship ($r = 0.94$, $R^2 = 0.86$). Under DS20 at the same altitude, GLI at FF remained significantly correlated with SW ($r = 0.89$, $R^2 = 0.72$), suggesting that vegetation indices retained substantial predictive capacity across sowing methods and flight altitudes.

Hence, the results demonstrated that vegetation indices derived from UAV imagery were highly effective in estimating biomass and yield-related traits, particularly FW and SW. Among the evaluated indices, GLI and NGRDI consistently produced the strongest relationships, especially during the full flowering stage under drill-seeded conditions. In addition, UAV flights conducted at 30–50 m generally yielded stronger correlations than those acquired at 60 m, highlighting the importance of flight altitude optimization for improving spectral sensitivity and crop trait prediction accuracy. The stronger relationships observed under drill seeding further suggest that uniform crop establishment enhanced canopy structure detection and improved the reliability of UAV-based phenotyping approaches.

Discussion

This study demonstrated that the performance of UAV-derived RGB vegetation indices (VIs) in predicting biomass and yield traits of common buckwheat was strongly dependent on the interaction among growth stage, sowing method, and UAV flight altitude. The variability in model performance across treatments indicates that VI-based crop monitoring is determined not only by spectral sensitivity but also by canopy architecture, spatial crop arrangement, and phenological dynamics that influence canopy reflectance patterns.

Among the evaluated flight altitudes, 50 m consistently produced the strongest correlations between VIs and biomass-related traits, particularly fresh weight (FW) and seed weight (SW). This superior performance likely reflects an optimal balance between spatial resolution and radiometric stability. At lower altitudes (30 m), UAV imagery provides finer canopy detail; however, excessive spatial heterogeneity, shadow effects, and within-canopy variability may increase spectral noise, reducing model consistency. In contrast, imagery acquired at 50 m likely minimized local canopy irregularities while still maintaining sufficient spatial resolution to detect vegetation greenness and biomass variation. Similar altitude-dependent improvements have been reported in UAV-based crop monitoring studies, where intermediate flight heights enhanced canopy aggregation and improved prediction accuracy by reducing pixel-level variability [5]. Conversely, the weaker relationships observed at 60 m suggest that increased flight altitude reduced canopy texture resolution and spectral sensitivity, thereby limiting the ability of RGB indices to distinguish subtle differences in plant vigor and biomass accumulation.

The stronger VI–trait relationships observed under drill seeding (DS20) compared with broadcast seeding (BS) further highlight the importance of canopy uniformity in UAV-based phenotyping. Drill seeding creates a more structured and homogeneous canopy arrangement, improving row continuity and reducing irregular gaps between plants. This spatial consistency likely enhanced the spectral response captured by RGB sensors, resulting in more stable and accurate VI estimations. In contrast, broadcast seeding produces irregular plant distribution and variable canopy density, which may increase background soil interference and reduce the consistency of reflectance signals. The improved correlations under DS20, therefore, suggest that UAV-derived indices are highly sensitive to canopy geometry and spatial organization rather than biomass alone. Similar observations have been reported in precision agriculture studies where crop establishment uniformity significantly improved remote sensing performance and vegetation index reliability [37].

The growth stage also played a critical role in determining model performance. At the third leaf (TL) stage, strong correlations between RGB-based indices and biomass traits were observed primarily under BS conditions. During early vegetative growth, canopy reflectance is dominated by leaf greenness, chlorophyll concentration, and canopy expansion, allowing RGB-based indices such as ExG, GLI, and NGRDI to effectively capture differences in plant vigor. Early-stage vigor is closely linked to photosynthetic capacity and nutrient uptake efficiency, which may explain why FW and even reproductive traits such as the number of seeds (NS) showed associations with TL-stage indices. Previous studies have similarly demonstrated that early vegetative vigor contributes substantially to stand establishment and eventual yield formation in buckwheat and other short-duration crops [18, 19, 43]. However, the predictive strength of early-stage models should be interpreted cautiously because reproductive success in buckwheat is also highly influenced by environmental conditions, pollination efficiency, and flowering synchronization [15, 44–46]. Thus, while early vigor provides valuable physiological information, it does not guarantee final yield stability.

At the full flowering (FF) stage, the strongest VI–trait relationships were predominantly observed under DS20, particularly for FW and SW. This stage-dependent improvement under drill seeding may reflect enhanced canopy closure and more uniform floral distribution. Nevertheless, flowering introduces substantial spectral complexity in buckwheat due to the abundance of white flowers, which can interfere with green-band reflectance and reduce the sensitivity of RGB-based vegetation indices. Earlier UAV studies conducted exclusively during

peak flowering reported weak or even negative correlations between green-based indices and biomass because floral reflectance masked canopy greenness signals [8, 13]. In the present study, however, significant correlations were still maintained during FF, particularly under DS20, suggesting that optimized sowing geometry and appropriate flight altitude partially mitigated floral interference effects. This finding emphasizes that model performance depends not only on crop phenology but also on the interaction between canopy structure and imaging conditions.

Among the evaluated indices, ExG and GLI showed more stable and consistent performance across altitudes and sowing methods than NGRDI. This may be because ExG and GLI are more sensitive to chlorophyll-driven canopy greenness and less affected by illumination variability and soil background reflectance. Their stronger performance indicates that indices emphasizing the green spectral component are particularly suitable for monitoring broadleaf crops such as buckwheat during vegetative development. In contrast, NGRDI performance appeared more variable across stages and treatments, suggesting greater sensitivity to canopy saturation and background effects. These findings indicate that VI selection should be tailored to crop phenology and canopy characteristics rather than assuming universal applicability of a single index.

The differing responses of biomass and yield traits also provide important biological insights. Fresh weight consistently showed stronger correlations with VIs than number of seeds (NS), indicating that spectral indices are more directly linked to vegetative biomass accumulation than reproductive output. Biomass traits are closely associated with canopy greenness, leaf area, and photosynthetic activity, all of which strongly influence RGB reflectance patterns. In contrast, reproductive traits such as seed production are governed by more complex physiological processes, including assimilate partitioning, flowering success, and stress tolerance, which may not be fully captured by canopy spectral information alone. The weaker correlations for NS therefore suggest that reproductive performance depends on additional factors beyond canopy vigor detectable by RGB imagery.

Although the present study demonstrated strong predictive potential using RGB-based UAV imagery, reliance solely on spectral indices remains a limitation. RGB indices primarily capture surface canopy greenness and may not fully represent structural crop attributes such as canopy height, biomass density, or lodging resistance. Integrating structural parameters derived from structure-from-motion (SfM) approaches, including canopy height models and canopy cover metrics, could substantially improve prediction robustness [10, 47, 48]

Furthermore, one limitation of this study is that it was conducted using a single buckwheat cultivar ('Yangjeol'), in one growing season, and at a single location. Therefore, the findings may not fully represent genotype × environment interactions across different cultivars, climatic conditions, or agro-ecological zones. Further multi-season, multi-location, and multi-varietal studies are required to validate the robustness and transferability of the proposed UAV-based vegetation index models. More broadly, the present study demonstrated that a single-dimensional factor cannot capture significant associations. It highlights that integrating optimized UAV operational parameters with agronomic configurations enhances the precision of remote sensing-based yield prediction. A multi-factor optimization approach, such as combining appropriate UAV altitude, sowing density, vegetation index (VI) selection, and phenological timing, is essential for developing accurate and transferable UAV-based crop monitoring models in precision agriculture.

Conclusion

This study demonstrates that the effectiveness of RGB-based UAV vegetation indices for estimating buckwheat growth and yield components is strongly dependent on phenological stage, sowing configuration, and flight altitude. Significant VI-trait relationships were identified primarily at the third leaf stage under broadcast seeding and at full flowering under drill seeding at 20 cm spacing, with 50 m emerging as the most consistently reliable flight altitude. Among the evaluated indices, ExG and GLI showed comparatively stable detection performance across conditions, whereas NGRDI exhibited more variable associations. The results further indicate that sowing method and spacing strongly modulate canopy structure, which in turn affects the strength of UAV-derived spectral relationships with ground-measured traits. Importantly, no single index, altitude, or agronomic configuration universally optimized prediction accuracy across all conditions. This highlights the necessity of integrated optimization of UAV operational parameters and crop management practices rather than reliance on a single standardized imaging setup. Thereby, these findings provide a practical framework for improving the reliability and transferability of RGB-based UAV monitoring systems in buckwheat production and precision agriculture.

Abbreviations

DS – 40	Drill Seeding at 40 × 5 cm spacings
DS – 30	Drill Seeding at 30 × 5 cm spacings
DS – 20	Drill Seeding at 20 × 5 cm spacings
DS – 12.5	Drill Seeding at 12.5 × 5 cm spacings
BS	Broadcast Seeding
FW	Total fresh weight of plants
SW	Seed weight
NS	Number of seeds per plant

PH Plant height

Supplementary Information

The online version contains supplementary material available at https://doi.org/10.1186/s12870-026-09427-4.

Supplementary Material 1.

Acknowledgements
Not Applicable.

Authors' contributions
E.M.B.M.K and S.M: Writing – original draft, Data curation. **S.M., E.M.B.M.K., T.N.N., HTTN., P.K., S.V and G.Y.D:** Methodology, Resources, Formal analysis and Validation. **M.C.D and Y.S.C** Conceptualization, Writing – review and editing, Funding acquisition, Supervision.

Funding
This research was supported by the Korea Institute of Marine Science & Technology Promotion (KIMST) funded by the Ministry of Oceans and Fisheries, Korea (RS-2025–02303933). This work was also supported by the Basic Science Research Program through the National Research Foundation of Korea (2017R1D1A1B06034883).

Data availability
Data will be made available on request.

Declarations

Ethics approval and consent to participate
Not applicable.

Consent for publication
Not applicable.

Competing interests
The authors declare no competing interests.

Author details
[1]Department of Plant Resources and Environment, Jeju National University, Jeju 63243, Republic of Korea
[2]Department of Horticulture, Faculty of Agriculture, Recep Tayyip Erdoğan University, Rize 53300, Türkiye
[3]Agricultural Digital Center, Jeju Special Self-Governing Province Agricultural Research and Extension Services, Jeju 63122, Republic of Korea
[4]Biology and Agriculture Lab, Department of Practical Arts Education, Cheongju National University of Education, Cheongju 28690, Republic of Korea
[5]Group of Applied Research in Advanced Materials for Sustainable Development, Faculty of Applied Sciences, Ton Duc Thang University, Ho Chi Minh City 700000, Vietnam
[6]Faculty of Applied Sciences, Ton Duc Thang University, Ho Chi Minh City 700000, Vietnam
[7]Department of Agronomy, Faculty of Agriculture, Kasetsart University, 50 Ngam Wong Wan Road, Chatuchak, Bangkok 10900, Thailand
[8]Department of Genetics, Faculty of Science, Kasetsart University, 50 Ngam Wong Wan Road, Chatuchak, Bangkok 10900, Thailand
[9]Institute of Theoretical and Applied Research, Duy Tan University, Hanoi 100000, Vietnam
[10]College of Medicine and Pharmacy, Duy Tan University, Da Nang 550000, Vietnam
[11]Department of Horticulture and Landscape Gardening, Faculty of Agriculture and Plantation Management, Wayamba University of Sri Lanka, Makandura, Gonawila 60170, Sri Lanka
[12]Environment and Life Sciences Programme, Faculty of Science, Universiti Brunei Darussalam, Jalan Tungku Link, Gadong BE1410, Negara Brunei Darussalam

Received: 7 March 2026 / Accepted: 29 June 2026
Published online: 08 July 2026

References

1. Di Gennaro SF, Nati C, Dainelli R, Pastonchi L, Berton A, Toscano P, et al. An Automatic UAV Based Segmentation Approach for Pruning Biomass Estimation in Irregularly Spaced Chestnut Orchards. Forests. 2020;11:308. https://doi.org/10.3390/f11030308.
2. Kazemi F, Parmehr EG. Evaluation of RGB vegetation incides derived from UAV images for rice crop growth monitoring. ISPRS Ann Photogramm Remote Sens Spat Inf Sci. 2023;X-4/W1-2022:385–90. https://doi.org/10.5194/isprs-annals-X-4-W1-2022-385-2023.
3. Lukas V, Huňady I, Kintl A, Mezera J, Hammerschmiedt T, Sobotková J, et al. Using UAV to identify the optimal vegetation index for yield prediction of oil seed rape (Brassica napus L.) at the Flowering Stage. Remote Sens. 2022;14:4953. https://doi.org/10.3390/rs14194953.
4. Jang GJ, Kim J, Yu JK, Kim HJ, Kim Y, Kim DW, et al. Review: cost-effective unmanned aerial vehicle (UAV) platform for field plant breeding application. Remote Sens. 2020;12:998. https://doi.org/10.3390/rs12060998.
5. Kwon S-H, Ku KB, Le AT, Han GD, Park Y, Kim J, et al. Enhancing citrus fruit yield investigations through flight height optimization with UAV imaging. Sci Rep. 2024;14:322. https://doi.org/10.1038/s41598-023-50921-8.
6. Mesas-Carrascosa F-J, Torres-Sánchez J, Clavero-Rumbao I, García-Ferrer A, Peña J-M, Borra-Serrano I, et al. Assessing Optimal Flight Parameters for Generating Accurate Multispectral Orthomosaicks by UAV to Support Site-Specific Crop Management. Remote Sens. 2015;7:12793–814. https://doi.org/10.3390/rs71012793.
7. Jin X, Liu S, Baret F, Hemerlé M, Comar A. Estimates of plant density of wheat crops at emergence from very low altitude UAV imagery. Remote Sens Environ. 2017;198:105–14. https://doi.org/10.1016/j.rse.2017.06.007.
8. Karunathilake EMBM, Tuan Thai T, Mansoor S, Le AT, Baloch FS, Chung YS, et al. Limitation of RGB-derived vegetation indices using UAV imagery for biomass estimation during buckwheat flowering. Phyton. 2025;94:2215–28. https://doi.org/10.32604/phyton.2025.067439.
9. Luo S, Jiang X, Yang K, Li Y, Fang S. Multispectral remote sensing for accurate acquisition of rice phenotypes: Impacts of radiometric calibration and unmanned aerial vehicle flying altitudes. Front Plant Sci. 2022;13:958106. https://doi.org/10.3389/fpls.2022.958106.
10. Golabi M, Lak S, Gilani A, Fazel MA, Egdernezhad A. Effect of sowing date and planting method on yield and yield components of three varieties of quinoa (Chenopodium quinoa Willd). Ital J Agron. 2024;19:100013. https://doi.org/10.4081/ija.2024.2212.
11. Awais M, Li W, Cheema MJM, Hussain S, AlGarni TS, Liu C, et al. Remotely sensed identification of canopy characteristics using UAV-based imagery under unstable environmental conditions. Environ Technol Innov. 2021;22:101465. https://doi.org/10.1016/j.eti.2021.101465.
12. Danilevicz MF, Bayer PE, Boussaid F, Bennamoun M, Edwards D. Maize Yield Prediction at an Early Developmental Stage Using Multispectral Images and Genotype Data for Preliminary Hybrid Selection. Remote Sens. 2021;13:3976. https://doi.org/10.3390/rs13193976.
13. Karunathilake EMBM, Thai TT, Mansoor S, Le AT, Baloch FS, Chung YS, et al. The use of RGB vegetation indices to predict the buckwheat yield at the flowering stage: (RGB Vegetation Indices for Yield Prediction During Flowering). J Crop Sci Biotechnol. 2025. https://doi.org/10.1007/s12892-025-00283-6.
14. Sulik JJ, Long DS. Spectral indices for yellow canola flowers. Int J Remote Sens. 2015;36:2751–65. https://doi.org/10.1080/01431161.2015.1047994.
15. Ji Z, Pan Y, Zhu X, Wang J, Li Q. Prediction of Crop Yield Using Phenological Information Extracted from Remote Sensing Vegetation Index. Sensors. 2021;21:1406. https://doi.org/10.3390/s21041406.
16. Turuu M, Sanjaakhand B, Bold O. Optimal UAV flight altitude for multispectral monitoring of wheat growth in Bayantsogt, Mongolia. Proc Mong Acad Sci. 2025:13–28. https://doi.org/10.5564/pmas.v65i02.4390.
17. Nijland W, De Jong R, De Jong SM, Wulder MA, Bater CW, Coops NC. Monitoring plant condition and phenology using infrared sensitive consumer grade digital cameras. Agric For Meteorol. 2014;184:98–106. https://doi.org/10.1016/j.agrformet.2013.09.007.
18. Arduini I, Masoni A, Mariotti M. A growth scale for the phasic development of common buckwheat. Acta Agric Scand Sect B — Soil Plant Sci. 2016;66:215–28. https://doi.org/10.1080/09064710.2015.1087587.
19. Campbell CG. Buckwheat, *Fagopyrum esculentum* Moench. Rome: IPGRI; 1997.

20. Song E. To spread the domestic variety "Yangjeol" 'It's the 2nd season and the harvest is 15% higher.' Maeil Business. 20244/8.
21. Reddy PS, Surendran R, Divya K, Raveena S, Selvaperumal SK, Lakshamanan R. Accuracy analysis and comparison of crop yield prediction using NB algorithm and RNN. Kuala Lumpur, Malaysia. 2024: 020363. https://doi.org/10.1063/5.0229471.
22. Balaji K V, Balamurugan KS, Thanarajan T, Selvi Sundarapandi AM. Machine learning-based crop recommendation system integrating soil properties and weather conditions with iot-driven data collection. Agrociencia. 2026:1–17. https://doi.org/10.47163/agrociencia.v60i1.3428.
23. Vinayagam J, Baskar D, Thanarajan T, Rajamanickam M. Blockchain-based crop monitoring using an interplanetary file system. Agrociencia. 2025;:1–15. https://doi.org/10.47163/agrociencia.v59i8.3553.
24. Shoba B, Kartheesan L, Priyanka SA, Deepa R, Surendran R. Quantum-driven agricultural innovation: evaluating wheat flour quality through thermal imaging and biophotonic emissions. In: 2025 3rd International Conference on Data Science and Network Security (ICDSNS). Tiptur, India: IEEE; 2025. p. 1–6. https://doi.org/10.1109/ICDSNS65743.2025.11168573.
25. Alkhafaji MA, Ramadan GM, Jaffer Z, Jasim L. Revolutionizing agriculture: the impact of AI and IoT. E3S Web Conf. 2024;491:01010. https://doi.org/10.1051/e3sconf/202449101010.
26. Soulaimani Y, Károly N. Integrating blockchain technology with internet of things. 12.
27. Agüera-Vega F, Carvajal-Ramírez F, Martínez-Carricondo P. Accuracy of digital surface models and orthophotos derived from unmanned aerial vehicle photogrammetry. J Surv Eng. 2017;143:04016025. https://doi.org/10.1061/(ASCE)SU.1943-5428.0000206.
28. Guillaume H. Drone legislation in South Korea: the essential guide. Drone and Cam. 2025. https://droneandcam.com/en/. Accessed 2 Mar 2026.
29. Davies ER. Image transformations and camera calibration. In: Computer vision. Elsevier; 2018. p. 585–610. https://doi.org/10.1016/B978-0-12-809284-2.00019-8.
30. Lee S, Lee S, Choi J. Correction of radial distortion using a planar checkerboard pattern and its image. IEEE Trans Consum Electron. 2009;55:27–33. https://doi.org/10.1109/TCE.2009.4814410.
31. Shin T, Jeong S, Ko J. Development of a Radiometric Calibration Method for Multispectral Images of Croplands Obtained with a Remote-Controlled Aerial System. Remote Sens. 2023;15:1408. https://doi.org/10.3390/rs15051408.
32. Ku KB, Mansoor S, Han GD, Chung YS, Tuan TT. Identification of new cold tolerant Zoysia grass species using high-resolution RGB and multi-spectral imaging. Sci Rep. 2023;13:13209. https://doi.org/10.1038/s41598-023-40128-2.
33. Cavalcanti VP, Dos Santos AF, Rodrigues FA, Terra WC, Araújo RC, Ribeiro CR, et al. Use of RGB images from unmanned aerial vehicle to estimate lettuce growth in root-knot nematode infested soil. Smart Agric Technol. 2023;3:100100. https://doi.org/10.1016/j.atech.2022.100100.
34. Jang G, Choi NJ, Wen J. Dual Nature of Paddy Field Lodging: A Unmanned Aerial Vehicle -Based Perspective. Korean J Crop Sci. 2024;69:209–15. https://doi.org/10.7740/kjcs.2024.69.4.209.
35. Soontranon N, Srestasathiern P, Rakwatin P. Rice growing stage monitoring in small-scale region using ExG vegetation index. In: 2014 11th International Conference on Electrical Engineering/Electronics, Computer, Telecommunications and Information Technology (ECTI-CON). Nakhon Ratchasima, Thailand: IEEE; 2014. p. 1–5. https://doi.org/10.1109/ECTICon.2014.6839830.
36. Zhang L, Zhang H, Han W, Niu Y, Chávez JL, Ma W. The mean value of gaussian distribution of excess green index: A new crop water stress indicator. Agric Water Manag. 2021;251:106866. https://doi.org/10.1016/j.agwat.2021.106866.
37. Silva AV, Silva CM, Silva JHB, Pereira WE, Albuquerque MB, Medeiros JC, et al. Remote sensing in maize: effect of vegetal biostimulants application in three stages of development. Braz J Biol. 2024;84:e279435. https://doi.org/10.1590/1519-6984.279435.
38. Wickham H, Averick M, Bryan J, Chang W, McGowan L, François R, et al. Welcome to the Tidyverse. J Open Source Softw. 2019;4:1686. https://doi.org/10.21105/joss.01686.
39. Kassambara A. ggpubr: "ggplot2" Based Publication Ready Plots. 2016:0.6.1. https://doi.org/10.32614/CRAN.package.ggpubr.
40. Fox J, Weisberg S. An R companion to applied regression. 2nd edition. Los Angeles London New Delhi Singapore Washington DC: Sage; 2011.
41. Schloerke B, Cook D, Larmarange J, Briatte F, Marbach M, Thoen E, et al. GGally: Extension to "ggplot2." 2010:2.4.0. https://doi.org/10.32614/CRAN.package.GGally.
42. de Mendiburu F. Agricolae: Statistical procedures for agricultural research. 2019;:1.3–7. https://doi.org/10.32614/CRAN.package.agricolae.
43. Worthing M, Mills A, McKenzie-Gopsill A. Reduced canopy cover and development compromises weed suppression by buckwheat in cover crop mixtures. Can J Plant Sci. 2025;105:1–5. https://doi.org/10.1139/cjps-2024-0117.
44. Rangappa K, Kumar A, U. Choudhury B, Moirangthem P, Layek J, Rajkhowa D, et al. Buckwheat: potential stress-tolerant crop for mid-hills of eastern himalaya under changing climate. In: Y. Waisundara V, editor. Agricultural Sciences. IntechOpen; 2024. https://doi.org/10.5772/intechopen.112096.
45. Dobbs AM, Ginn D, Skovsen SK, Yadav R, Jha P, Bagavathiannan MV, et al. Using structure-from-motion to estimate cover crop biomass and characterize canopy structure. Field Crops Res. 2023;302:109099. https://doi.org/10.1016/j.fcr.2023.109099.
46. Xie J, Zhou Z, Zhang H, Zhang L, Li M. Combining Canopy Coverage and Plant Height from UAV-Based RGB Images to Estimate Spraying Volume on Potato. Sustainability. 2022;14:6473. https://doi.org/10.3390/su14116473.
47. Koyama T, Suenaga M, Takeshima R. Growth and yield response of common buckwheat (*Fagopyrum esculentum* Moench) to waterlogging at different vegetative stages. Plant Prod Sci. 2019;22:456–64. https://doi.org/10.1080/1343943X.2019.1670682.
48. Ali-Khan ST. Effect of Row Spacing and Seeding Rate on Yield of Buckwheat[1]. Agron J. 1973;65:914–5. https://doi.org/10.2134/agronj1973.00021962006500060020x.

Publisher's Note

Springer Nature remains neutral with regard to jurisdictional claims in published maps and institutional affiliations.